

An alternative splice variant of human α A-crystallin modulates the oligomer ensemble and the chaperone activity of α -crystallins

Waldemar Preis¹ · Annika Bestehorn¹ · Johannes Buchner¹ · Martin Haslbeck¹

Received: 6 December 2016 / Revised: 31 January 2017 / Accepted: 1 February 2017 / Published online: 18 February 2017
© Cell Stress Society International 2017

Abstract In humans, ten genes encode small heat shock proteins with lens α A-crystallin and α B-crystallin representing two of the most prominent members. The canonical isoforms of α A-crystallin and α B-crystallin collaborate in the eye lens to prevent irreversible protein aggregation and preserve visual acuity. α -Crystallins form large polydisperse homo-oligomers and hetero-oligomers and as part of the proteostasis system bind substrate proteins in non-native conformations, thereby stabilizing them. Here, we analyzed a previously uncharacterized, alternative splice variant (isoform 2) of human α A-crystallin with an exchanged N-terminal sequence. This variant shows the characteristic α -crystallin secondary structure, exists on its own predominantly in a monomer–dimer equilibrium, and displays only low chaperone activity. However, the variant is able to integrate into higher order oligomers of canonical α A-crystallin and α B-crystallin as well as their hetero-oligomer. The presence of the variant leads to the formation of new types of higher order hetero-oligomers with an overall decreased number of subunits and enhanced chaperone activity. Thus, alternative mRNA splicing of human α A-crystallin leads to an additional, formerly not characterized α A-crystallin species which is able to modulate the properties of the canonical ensemble of α -crystallin oligomers.

Keywords Alpha-crystallin · Alternative splicing · Protein folding · Chaperone function · sHsp

Introduction

The two homologous, vertebrate proteins α A-crystallin and α B-crystallin are members of the small heat shock protein (sHSP) family. Both proteins represent a major component of the vertebrate eye lens, and together with β -crystallins and γ -crystallins, they constitute approximately 90% of all proteins in the lens (Bassnett et al. 2011; Bloemendal et al. 2004; Clark et al. 2012). Additionally, α B-crystallin is constitutively expressed in a wide variety of tissues such as the brain, cardiac and skeletal muscles, and kidney (Bhat and Nagineni 1989; Dubin et al. 1989; Iwaki et al. 1990; Iwaki et al. 1989; Kato et al. 1991b). In contrast α A-crystallin is found mainly in the eye lens (Robinson and Overbeek 1996) and only in minor amounts in other tissues like the spleen, heart, and thymus (Kato et al. 1991a; Srinivasan et al. 1992). Functionally, the ensemble of both α -crystallins is involved in maintaining eye lens transparency (Bassnett et al. 2011; Bloemendal et al. 2004; Clark et al. 2012; Delaye and Tardieu 1983; Jaenicke and Slingsby 2001; Tardieu 1988). The eye lens represents an environment with an exceptionally high protein concentration of up to ~450 mg/mL (Fagerholm et al. 1981; Siezen et al. 1988) and little or no protein turnover (Hoehenwarter et al. 2006; Wistow and Piatiogorsky 1988). Throughout lens development and aging, lens proteins go through covalent and non-covalent modifications and become progressively susceptible for aggregation and unfolding. α -Crystallins are thought to bind these fragile, non-native proteins and protect them from irreversible aggregation by means of their chaperone activity, ensuring proper light refraction and visual acuity. Both α -crystallins were found in vitro to

Electronic supplementary material The online version of this article (doi:10.1007/s12192-017-0772-2) contains supplementary material, which is available to authorized users.

✉ Martin Haslbeck
martin.haslbeck@tum.de

¹ Department Chemie, Center for Integrated Protein Science, Technische Universität München, Lichtenbergstrasse 4, 85748 Garching, Germany

inhibit thermal aggregation (Horwitz 1992; Horwitz 1993; Jakob et al. 1993), aggregation induced by the reduction of disulfide bonds (Bhattacharyya and Das 1998; Raman et al. 1995), and high-energy electromagnetic radiation like UV light (Bhattacharyya and Das 1998; Raman and Rao 1994; Reddy et al. 2001). Dysfunctions caused by mutations, degradation, or unspecific post-translational modifications lead to lens opacification, clinically termed cataract (Clark et al. 2012). One characteristic feature of sHsps and α -crystallins is to form ensembles of large homo-oligomeric and hetero-oligomeric complexes that are polydisperse and dynamic. Subunit exchange between different sHSPs in vitro and in vivo further contributes to ensemble complexity and variation of properties (Bova et al. 1997; Haslbeck et al. 2016; Kundu et al. 2007). The ability to form these dynamic ensembles also is closely correlated to the chaperone activity of sHsps and α -crystallins. In this context, a variety of co-translational and post-translational modifications (PTMs), with phosphorylation being one of the most prominent, have been shown to influence the ensemble composition and its activity (Hoehenwarter et al. 2006; Peschek et al. 2013). Structurally, α -crystallins exhibit a tripartite domain organization with a central conserved α -crystallin domain (ACD) flanked by less conserved N-terminal (NTS) and C-terminal sequences (CTS). The ACD represents the signature motif of all sHSPs and comprises ~80 amino acids in human α -crystallins. It contains predominantly β -sheet structures forming an immunoglobulin-like β sandwich (Laganowsky et al. 2010; Laganowsky and Eisenberg 2010). The NTS of human α A-crystallin and α B-crystallin consists of 63 and 67 amino acids, respectively. While it remains elusive which structural elements are present in the NTS of α A-crystallin, for α B-crystallin, the first five residues were proposed to be highly flexible, and based on ssNMR and secondary structure prediction, it was proposed that the NTS includes three short α -helices and a short β -strand connected by long unstructured linkers (Braun et al. 2011; Carver et al. 1992; Jehle et al. 2011). Interestingly, the NTS of both α -crystallins displays high hydrophobicity and conformational mobility and is essential for higher order oligomer assembly (Eifert et al. 2005; Haslbeck et al. 2005; Jehle et al. 2011). N-terminally truncated mutants of bovine α B-crystallin form more heterogeneous ensembles of oligomers which contain overall a lower number of subunits than the oligomers formed by the full-length protein. NTS-depleted rat (Merck et al. 1992; Merck et al. 1993), bovine (Eifert et al. 2005; Laganowsky et al. 2010; Salerno et al. 2003), and human (Berengian et al. 1999; Bova et al. 2000; Kundu et al. 2007) α A-crystallin forms dimers and preferentially tetramers. Furthermore, the chaperone activity of the NTS-depleted mutants is lower than that of the full-length protein (Kundu et al. 2007; Laganowsky et al. 2010; Mainz et al. 2015; Merck et al. 1993).

Intriguingly, alternative RNA splicing of α -crystallin as a co-transcriptional and post-transcriptional process has not yet been investigated in detail. The two human genes CRYAA and CRYAB are the result of a gene duplication event of an ancestral α -crystallin gene leading to isoforms with 173 and 175 amino acids, respectively. For α A-crystallin, in rodents (Cohen et al. 1978a; Cohen et al. 1978b; de Jong et al. 1980) and certain mammals like hedgehog, bat, and pika (Hendriks et al. 1988), an alternative splice variant termed α A^{ins} with decreased chaperone activity (Derham et al. 2001) was identified. This variant is identical to α A-crystallin but has an additional “insert exon” located in the first intron, resulting in 23 additional amino acids between the NTS and ACD (King and Piatigorsky 1983; van den Heuvel et al. 1985). In primates however, the analogous exon probably developed to a pseudo-exon 30 to 40 myr ago and is in the early stages of being extinguished (Jaworski and Piatigorsky 1989).

In humans, the canonical isoform 1 of both α A-crystallin and α B-crystallin is encoded by three exons. The last two exons correspond to the ACD and the CTS. The first exon codes for the respective NTS (Graw 2009). For α B-crystallin, the Ensemble database (Release 86, October 2016) annotates several differential transcripts some of which are truncated at the 3' or 5' ends which prevent annotation of the complete coding sequence (CDS). Nevertheless, three transcripts are proposed to be protein coding. One is the canonical isoform with 175 aa. The others result in proteins with 155 aa (Transcript ID ENST00000533971.1) and 108 aa (Transcript ID ENST00000525823.1). The first variant originates from skipping of the splice site behind the second exon, therefore extending the second exon and terminating at a new stop codon. This would be a C-terminally shortened version of α B-crystallin changing the sequence of half of the ACD and the CTS. The second variant would lead to a skipping of the first exon, being equivalent to a truncation of the complete NTS.

Interestingly, for human α A-crystallin, only splice variants leading to substitutions of the NTS are predicted. Here, we describe the presence of an alternative splice variant of α A-crystallin with an alternative NTS in the lens tissue. We set out to analyze the structural and functional implications of the exchange of the NTS in this variant. Additionally, we show that the alternatively spliced α A-crystallin variant interacts with canonical human α -crystallins and modulates their oligomeric size and chaperone activity.

Materials and methods

Cloning, expression, and purification of α -crystallins

The synthetic gene (Thermo Fisher Scientific) for α A-crystallin isoform 1 was cloned in a pE-SUMOpro (Life Sensors) expression vector via BsaI and XbaI with an N-

terminal 6 \times His-SUMO tag. For purification, the plasmid containing α A-crystallin isoform 1 was introduced into the *Escherichia coli* strain BL21 cod+. Cultures were grown in LB medium at 37 °C until an A_{600} of \sim 0.6 was reached. Subsequently, 1 mM IPTG was added for induction of the protein expression. After 4 h of incubation at 37 °C, cells were harvested, washed, and resuspended in buffer A (40 mM $\text{NaH}_2\text{PO}_4/\text{Na}_2\text{HPO}_4$ pH 7.4, 500 mM NaCl, 20 mM imidazole, 1 mM DTT). Cell lysis was accomplished by passing the cell suspension through a Basic Z cell disruption system (Constant Systems) at 2.3 kbar. After centrifugation for 30 min at 48,000 $\times g$, urea was added to 3.5 M to the supernatant. The protein was purified via metal chelate chromatography on a 5-mL HisTrap FF column (GE Healthcare). The column was pre-equilibrated and after sample application washed with buffer A_{urea} (40 mM $\text{NaH}_2\text{PO}_4/\text{Na}_2\text{HPO}_4$ pH 7.4, 500 mM NaCl, 20 mM imidazole, 3.5 M urea, 1 mM DTT) and buffer B_{urea} (40 mM $\text{NaH}_2\text{PO}_4/\text{Na}_2\text{HPO}_4$ pH 7.4, 500 mM NaCl, 30 mM imidazole, 3.5 M urea, 1 mM DTT). The protein was eluted with buffer C_{urea} (40 mM $\text{NaH}_2\text{PO}_4/\text{Na}_2\text{HPO}_4$ pH 7.4, 500 mM NaCl, 300 mM imidazole, 3.5 M urea, 1 mM DTT). Fractions containing protein were pooled and dialysed into low salt buffer (50 mM MES pH 6, 3.5 M urea, 2 mM EDTA, 1 mM DTT). For further purification, the protein was loaded onto a RESOURCE S cation exchange column (GE Healthcare) and eluted with a gradient spanning 20 column volumes (CV) to high salt buffer (50 mM MES pH 6, 500 mM NaCl, 3.5 M urea, 2 mM EDTA, 1 mM DTT). The protein was dialysed into buffer A, and the His-SUMO tag was cleaved off with His-tagged SUMO protease (Bepperling et al. 2012). Following a second metal affinity chromatography to separate from the SUMO protease and the tag, the protein was dialysed into PBS containing 2 mM EDTA and 1 mM DTT and after concentration loaded onto a Superdex 200 pg gel filtration column (GE Healthcare). The α A-crystallin containing fractions were pooled, concentrated, frozen in liquid nitrogen, and stored at -80 °C. α A-crystallin isoform 2 was synthesized (Thermo Fisher Scientific) and cloned into a modified pET-28b expression vector with an N-terminal 6 \times His-SUMO tag (Bepperling et al. 2012) and expressed in BL21 cod+ in LB medium. The cells were grown at 37 °C until an A_{600} of \sim 0.6 was reached. Expression was induced with 0.1 mM IPTG, and the cells were incubated at 30 °C for 16 h after induction. Further purification steps were equivalent to isoform 1 except that no urea was used throughout the protein preparation. The eluted protein was dialysed into buffer A, and the His-SUMO tag was cleaved off with SUMO protease. The protein was loaded onto a nickel column, the flow through dialysed into 40 mM $\text{NaH}_2\text{PO}_4/\text{Na}_2\text{HPO}_4$ pH 6.8, 40 mM NaCl, 1 mM DTT, and purified with a RESOURCE S cation exchange

column (GE Healthcare) and a 20 CV gradient to 40 mM $\text{NaH}_2\text{PO}_4/\text{Na}_2\text{HPO}_4$ pH 6.8, 500 mM NaCl, 1 mM DTT as elution buffer. The eluted protein was dialysed into PBS with 2 mM EDTA and 1 mM DTT, concentrated, frozen in liquid nitrogen, and stored at -80 °C. α B-crystallin was purified as described elsewhere (Peschek et al. 2009).

Reverse transcription and PCR analysis of HLEpiC total RNA isolate

First-strand synthesis of cDNA of HLEpiC total RNA isolate (ScienCell) was accomplished with M-MLV RT (Promega) using oligo dT primers following the manufacturer's instructions. PCR amplification and sequencing (Eurofins Genomics) were performed with the primers listed in Table 1. Positions are indicated in Fig. 1a. GoTaq G2 polymerase (Promega) was used for PCR analysis.

Far-UV CD spectroscopy

Far-UV circular dichroism (CD) spectra of α -crystallins were recorded at room temperature using a Chirascan-plus CD spectrometer (Applied Photophysics) flushed with dry nitrogen. Spectra were collected from 260 to 195 nm in a 106-QS cuvette (Hellma) with 0.2-mm path length. The measurement time per data point was set to 0.7 s. Proteins were diluted in PBS with 2 mM EDTA and 1 mM DTT to a final concentration of 0.5 mg/mL and incubated at 37 °C for at least 1 h prior to analysis. The depicted spectra are the average of 10 individual scans. Savitsky–Golay smoothing was applied to spectra with a polynomial order of 3 and a smoothing window of 10 points. Spectra were deconvoluted using CDNN 2.1 (Bohm et al. 1992).

Analytical ultracentrifugation

Sedimentation velocity experiments were carried out with a ProteomLab XL-I (Beckman) equipped with absorbance optics. Cells with quartz windows and 12-mm path length were centrifuged at 42,000 rpm and 20 °C using an An-50 Ti rotor (Beckman). α A-crystallin isoform 2 was preincubated in PBS including 1 mM TCEP at 37 °C for at least 1 h prior to analysis. The signal was monitored at 230 nm. Data analysis was carried out in continuous $c(s)$ distribution mode of SEDFIT (Schuck 2000; Schuck 2003). For each concentration, a best fit frictional ratio was calculated and a consistent average value was used for calculation of $c(s)$ distributions. The area under each curve was normalized to 1.

Table 1 Primers used for nested RT-PCR measurements to verify the presence of different splice variants in HLEpiC total RNA isolate

Roman numbering	Sequence
I	5'-TGA CTC CTG CCA GCC TCC AG-3'
II	5'-CCC CGT GGT ACC AAA GCT GAA C-3'
III	5'-GGT CAT AGT CCT GAA AGC CAG AGA GC-3'
IV	5'-GGC GTT CCT AGC ACC TCC TCC-3'
V	5'-ATG AGC TCG GCC TGC CCA C-3'
VI	5'-ACC AGT AGC ATT CAG CCC CTC AG-3'
VII	5'-GGT TTG GAG ACA GGT CGA GGG TC-3'
VIII	5'-ATG CCT GTC TGT CCA GGA GAC AG-3'
IX	5'-AGC CGA GGC AAT GCC TGC-3'
X	5'-CAT GAT GGG CCA GGG CTG C-3'

Analytical size exclusion chromatography and precipitation

The apparent molecular mass of the individual α -crystallins and mixtures was measured by size exclusion chromatography. A Superdex 200 10/300 GL (GE Healthcare) analytical gel filtration column was applied at a constant flow rate of 0.5 mL/min at 20 °C. The column was equilibrated with PBS including 2 mM EDTA and 1 mM DTT. Proteins were preincubated at 37 °C for at least 1 h prior to analysis. For measurements of α A-crystallin isoform 2 alone, 5.2 nmol protein was loaded, while for measurements in mixtures with α A-crystallin and α B-crystallin isoform 1, 2.3 nmol of each protein was used. Since α A-crystallin isoform 2 does not contain a tryptophane residue, fluorescence at 303 nm with an excitation at 273 nm was recorded. The gel filtration standard (Bio-

Rad) was used for calibration. Proteins eluting from the column were fractionated, and the protein content was precipitated. In a 1:1000 ratio, a 10% sodium deoxycholic acid (NaDOC) solution was added, and the mixture was incubated on ice for 30 min. Trichloroacetic acid (TCA) was added to a final concentration of 10%, and the mixture was further incubated at 4 °C overnight. After centrifugation at 17,000 \times g, the pellet was resuspended in 2 \times SDS-PAGE loading dye and neutralized with 1 M Tris solution. Samples were applied to SDS-PAGE followed by western blotting if applicable. Immunodetection was conducted with a polyclonal rabbit antibody raised against α A-crystallin isoform 1 (Pineda Antikörper-Service) in a 1:10,000 dilution and peroxidase coupled anti-rabbit IgG (Sigma) in a 1:20,000 dilution. WesternBright ECL Spray (Advansta) was used as substrate solution for chemiluminescence detection with an

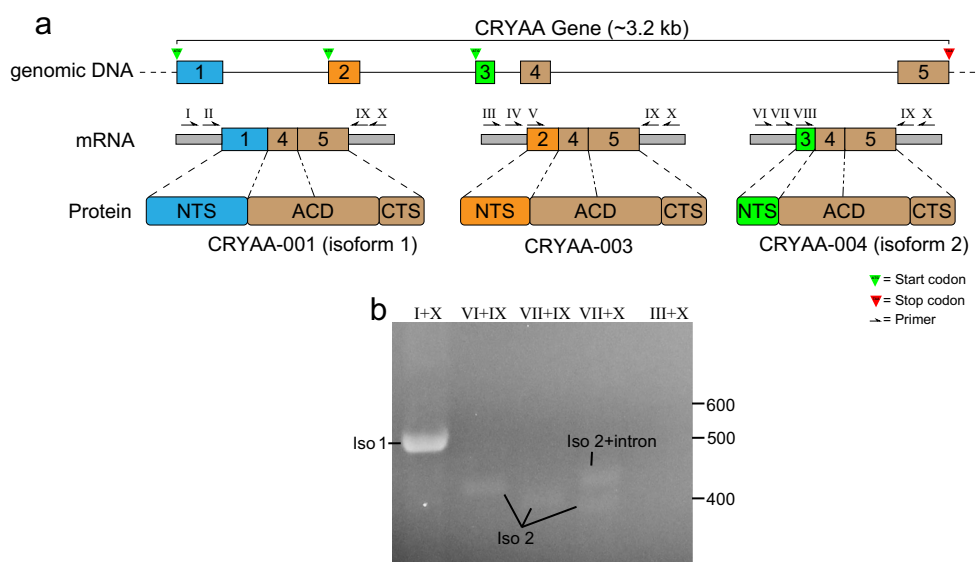


Fig. 1 Verification of an alternative splice variant of α A-crystallin in primary human lens epithelial cells. **a** The structure of the human CRYAA gene with the resulting transcripts and potential protein segmentation. Numbered boxes represent exons and the lines in between introns. Narrow gray boxes represent untranslated regions

(UTRs). N-terminal sequence (NTS) (blue, orange, and green), α -crystallin domain (ACD) and C-terminal sequence (CTS) (brown). Green and red triangles indicate start and stop codons. Half-headed and numbered arrows indicate primer positions. **b** Nested PCR analysis of cDNA preparations from HLEpiC cells

ImageQuant LAS 4000 (GE Healthcare). Signal bands were quantified with the 1D gel analysis function of the ImageQuant TL software (GE Healthcare). Where indicated, fluorescence signals and densities of western blot bands were normalized to the highest signal.

Multi-angle light scattering analysis

The molar masses (M) of the proteins were determined using a multi-angle light scattering (MALS) detector and Astra V software (Wyatt Technology). Prior to MALS analysis, protein samples were separated on a Superdex 200 5/150 GL (GE Healthcare) size exclusion column connected to an HPLC (Shimadzu) equipped with UV and RID detectors. PBS containing 2 mM EDTA and 1 mM DTT was used as running buffer, and the flow rate was set to 0.5 mL/min at 20 °C. The signal intensities of depicted differential refractive index peaks were normalized to one. Proteins were preincubated at 37 °C for at least 1 h prior to analysis. Each sample consisted of 30 μ L with a total protein concentration of 50 μ M. Mixtures of α -crystallins were in equimolar concentrations.

Chaperone activity

Chaperone activity of α -crystallins in terms of suppression of thermal aggregation of model substrates was determined using bovine L-malate dehydrogenase from pig heart (MDH, mitochondrial, Roche) at 42 °C and rhodanese from bovine liver (Sigma) at 45 °C as substrates. The substrate concentration was 2 μ M for MDH and 2 μ M for rhodanese, while α -crystallins were used in different ratios to substrates. Mixtures of α -crystallins were in equimolar concentrations. Absorbance was measured in at least triplicates at 360 nm in 105.201-QS cuvettes (Hellma) using an Ultrospec 3100 *pro* UV-Vis spectrometer (GE Healthcare). The assay buffer consisted of PBS with 2 mM EDTA and 1 mM DTT (Mymrikov et al. 2016), and proteins were preincubated at 37 °C for at least 1 h. Absorbance signals were normalized to the aggregation signals of the substrates in the absence of chaperone, setting the maximum A_{360} value achieved to 1. All measurements were repeated at least three times, and the mean values and standard deviations (SD) were calculated.

Results and discussion

Alternative splicing of the primary transcript results in differentially spliced variant of α A-crystallin

According to the Ensemble database (Release 86, October 2016), the gene CRYAA is predicted to produce up to five different splice products. One transcript does not contain an open reading frame, and one retains an intron, which renders it

unlikely to be further processed and translated. The other three splice products are predicted to be protein coding. All these potential protein-coding products consist of three exons after splicing, whereby the last two exons are identical in all splice products (Fig. 1a), indicating that five exons represent the building blocks to produce the potentially protein-coding splice variants. The first exon, however, is variable, and alternative use of three different versions of this exon might produce three different, protein-coding splice variants. Interestingly, the first exon codes for the complete NTS, respectively, the first 63 amino acids in isoform 1 which generate the common wild-type form of α A-crystallin. Exon 4 and exon 5 (Fig. 1a) of the variants encode roughly the first half of the ACD and the second half of the ACD including the CTS, respectively. Attachment of exon 1 leads to isoform 1 of α A-crystallin and the alternatively attached exons 2 and 3 to shorter isoforms with completely different NTS. The linkage of exon 3 leads to the shortest splice variant referred to as isoform 2 by NCBI (acc. no. NP_001307648; Supplementary Fig. 1), which was already identified in adult human retina and fetal eye tissue on the basis of expressed sequence tag analysis (Bonaldo et al. 1996; Graw 2009; Wistow et al. 2002). This indicates that isoform 2 has an expression profile similar to that of isoform 1. To verify these results, we first tested if the three potential protein-coding splice variants of α A-crystallin are present in the human eye lens.

In cultivated human lens epithelial cells, the expression of α A-crystallin decreases throughout passaging (Fleming et al. 1998; Lenstra et al. 1982). Therefore, we investigated the presence of all splice variants in primary epithelial cells. The total RNA isolate of these HLEpiC cells was reverse transcribed, and nested PCRs with varying primers were conducted (Fig. 1b, Table 1, and Supplementary Fig. 2). Using primers complementary to the UTR before exon 1 (I, II) and after exon 5 (IX; X) resulted in a strong band at ~600 bp corresponding to the isoform 1 of α A-crystallin, while targeting sequences close to or within exon 2 (III, IV, V) did not show any bands (Fig. 1b and Supplementary Fig. 2). With primers close to exon 3 (VI, VII), several bands developed. The bands were isolated and reamplified with primers binding closer to (VII) or inside of exon 3 (VIII) (Supplementary Fig. 2). Isolation and DNA sequence analysis of these fragments confirmed the band in lane 1 to be equivalent to the fused exons 1, 4, and 5, which corresponds to isoform 1. The upper band at ~500 bp comprises exons 3, 4, and 5 including the intron between exons 3 and 4. This demonstrates the presence of a splice product, which retains an intron matching the predicted CRYAA-005 (Transcript ID ENST00000468016.1) from the Ensemble database, which additionally includes several premature stop codons disabling synthesis of the respective α A-crystallin isoform on the protein level. On the other hand, the lower band at ~400 bp originates from the fused

exons 3, 4, and 5 representing α A-crystallin isoform 2. Aligning several human sHsps with this variant, we found that there are no highly conserved sites in the NTS of α A-crystallin isoform 2, but secondary structure prediction tools showed that potential α -helices are located in the NTS at positions similar to α A-crystallin and α B-crystallin isoform 1 (Supplementary Fig. 1). In addition, the hydrophobic properties in this segment turned out to be comparable (Supplementary Fig. 3a and b). Taken together, our results substantiate the presence of isoform 2 as an alternative splice variant in human lens epithelial cells, whereas we were not able to find evidence for the existence of CRYAA-003.

The splice variant α A-crystallin isoform 2 is a soluble and structured protein with high similarity to isoform 1

To compare the structural properties of α A-crystallin isoforms 1 and 2, we expressed and purified both variants and conducted far-UV CD measurements of both α A-crystallin isoforms and α B-crystallin isoform 1 (Fig. 2). The CD spectra show that α A-crystallin isoform 1 and isoform 2 represent folded proteins after purification. For both proteins, the spectra indicate a high β -sheet content with small amounts of α -helices which is characteristic for α -crystallins and other sHsps (Haslbeck et al. 2005; Liang et al. 1985). Deconvolution of the spectra revealed that isoform 1 has a slightly lower content of β -sheet (38% isoform 1 vs. 43% isoform 2) but a higher α -helical content (9% isoform 1 vs. 6% isoform 2) (Table 2). This indicates that the stable α -crystallin domain does not seem to be affected by the changes in the NTS. Additionally, the results are in agreement with previous results on NTS truncation mutants of α A-crystallin (Bova et al. 2000; Kundu et al. 2007; Merck et al. 1993) (Table 3).

α A-crystallin isoform 2 forms a monomer–dimer equilibrium

An important general feature of α -crystallins and other sHsps is that they are able to form polydisperse high molecular weight oligomers. In this context, it was proposed that the NTS includes one of the interaction sites necessary for the formation of higher oligomers (Delbecq and Kleivit 2013;

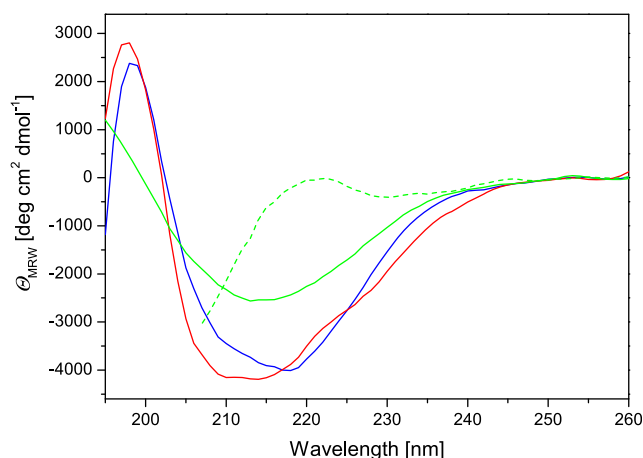


Fig. 2 Far-UV CD spectra of α -crystallins. The splice variant α A-crystallin isoform 2 (green line) is a soluble and structured protein with high similarity to isoform 1 of α A-crystallin (blue line) and α B-crystallin (red line). Addition of 5 M guanidine hydrochloride to α A-crystallin isoform 2 results in the loss of the secondary structure (green, dashed line)

Haslbeck et al. 2016). Therefore, we addressed the question whether the exchange to an alternative NTS in α A-crystallin isoform 2 affects its ability to form higher oligomers. To monitor the apparent molecular mass of the splice variant, we utilized size exclusion chromatography which revealed that the main peak eluting from the column is indicative for a monomer while a slightly earlier eluting side peak belongs to a dimer (Fig. 3a). Western blot analysis confirmed that the two peaks correspond to α A-crystallin isoform 2 (Fig. 3a and Supplementary Fig. 4), indicating an equilibrium between both states. To validate these results, we applied analytical ultracentrifugation (aUC) sedimentation velocity measurements. Interestingly, at low concentrations, only a monomer peak at 1.5 S was detected, but with increasing concentrations, dimers were observed at 2.3 S, which shows that α A-crystallin isoform 2 is in a monomer–dimer equilibrium. This observed trend of forming smaller oligomers after exchanging the NTS by a shorter, alternative version correlates to previous reports on truncations or deletions of the NTS of α A-crystallin which lead to dimer and tetramer formation in rat α A-crystallin (Merck et al. 1992). Similarly, N-terminally truncated bovine α A-crystallin was identified as a

Table 2 Deconvolution of far-UV CD spectra of α A-crystallin isoforms 1 and 2 and α B-crystallin isoform 1 using CDNN

Secondary structure element	α A isoform 1	α A isoform 2	α B isoform 1
Helix	7.9%	5.6%	11.5%
Antiparallel β -sheet	32.7%	37.6%	30.2%
Parallel β -sheet	5.5%	5.4%	5.7%
β -Turn	19.2%	19.3%	18.7%
Random coil	35.0%	35.0%	34.8%

Table 3 Calculated apparent molecular mass and number of subunits according to SEC and MALS measurements

Proteins	Apparent molecular mass (oligomer size) by SEC	Apparent molecular mass (oligomer size) by SEC-MALS
α A-crystallin isoform 1	516 kDa (~26)	458 kDa (~23)
α A-crystallin isoform 1 + 2	386 kDa	365 kDa
α B-crystallin	547 kDa (~27)	512 kDa (~25)
α B-crystallin + α A-crystallin isoform 2	431 kDa	461 kDa
α B-crystallin + α A-crystallin isoform 1	579 kDa	545 kDa
α B-crystallin + α A-crystallin isoform 1 + 2	489 kDa	523 kDa

predominant tetramer with minor dimer content (Eifert et al. 2005; Laganowsky et al. 2010; Salerno et al. 2003). In addition, the formation of higher oligomeric species was reported to be concentration dependent also for full-length α A-crystallin and some truncated variants (Laganowsky et al. 2010). Furthermore, removal of more than 20 residues from the NTS drastically reduces the oligomeric size of human α A-crystallin, and complete removal of the NTS resulted in the formation of a tetramer (Kundu et al. 2007). In the case of the splice variant, the further reduction of the complex size might be caused by the significant change in the charge state of the NTS. Assuming that the histidines are uncharged, the NTS of α A-crystallin isoform 1 has a predicted net charge of -2 , where isoform 2 has a total predicted charge of its shorter NTS of $+4$ (Supplementary Fig. 5). The charge variation in combination with the loss of the predicted α -helices, the alternative NTS seems to hinder α A-crystallin isoform 2 to form tetramers out of dimers and thus interferes with the assembly of higher order oligomers.

α A-crystallin isoform 2 shows decreased chaperone activity

Oligomer formation of sHsps commonly correlates directly with their chaperone activity, and the NTS is thought to be involved in the interaction with the substrate proteins. Hence, we next investigated if the alternative NTS of α A-crystallin isoform 2 modulates its activity. To test this, we measured the influence of α A-crystallin isoform 2 on the thermal denaturation of malate dehydrogenase (MDH) and rhodanese as model substrates. For MDH, no significant inhibition of the aggregation could be observed at substoichiometric ratios of α A-crystallin isoform 2/MDH (Fig. 4a, c). Chaperone activity was only observed when a molar excess of α A-crystallin isoform 2 was used, and complete inhibition was only reached at a ten-fold excess (Fig. 4b). For rhodanese, no suppression of the thermal aggregation by α A-crystallin isoform 2 could be achieved. These observations are in accordance with N-terminal and C-terminal truncations of bovine α A-crystallin

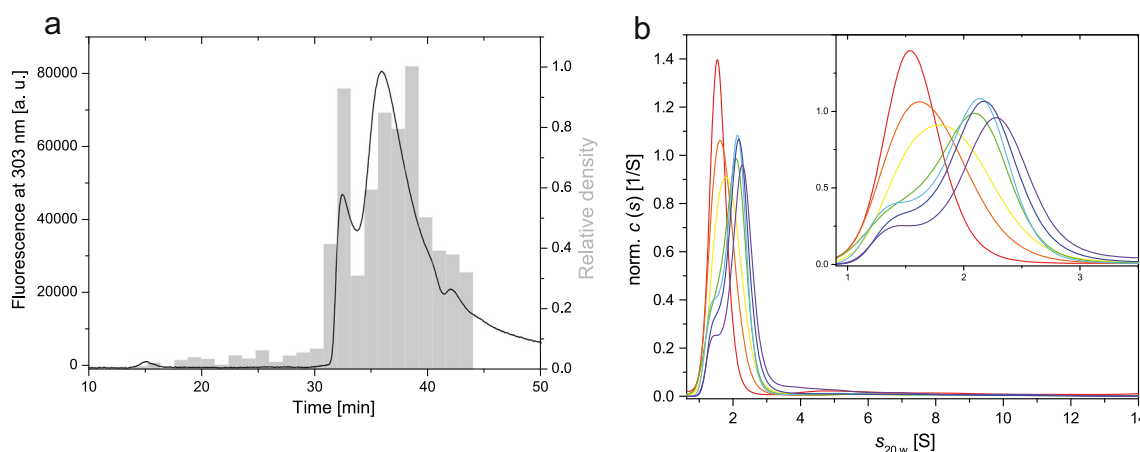


Fig. 3 α A-crystallin isoform 2 forms preferentially monomer and dimeric complexes. **a** SEC elution profile (black line) is overlaid with the relative density of the respective quantified western blot bands of precipitated fractions (gray bars). **b** Sedimentation velocity analysis of

α A-crystallin isoform 2 at 3 μ M (red line), 5 μ M (orange line), 7.5 μ M (yellow line), 10 μ M (green line), 12.5 μ M (light blue line), 15 μ M (dark blue line), and 20 μ M (purple line)

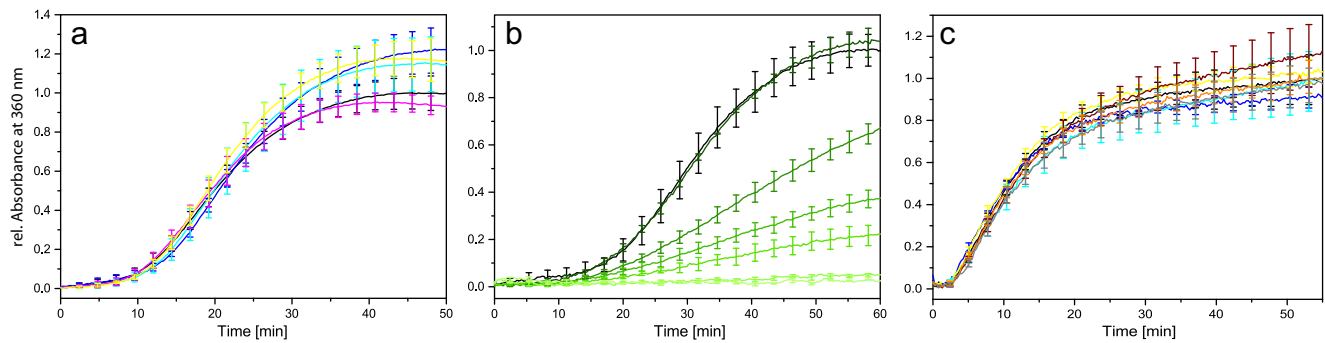


Fig. 4 α A-crystallin isoform 2 has a weak chaperone activity towards thermally denatured MDH and no chaperone activity towards rhodanese at close to equimolar concentrations. **a** MDH aggregation assay with α A-crystallin isoform 2 at 0 μ M (black line), 0.125 μ M (blue line), 0.25 μ M (cyan line), 0.375 μ M (magenta line), and 0.5 μ M (yellow line). **b** MDH

aggregation assay with α A-crystallin isoform 2 at 0, 2, 5, 8, 10, 20, and 40 μ M ranging from black to light green. **c** Rhodanese aggregation assay with α A-crystallin isoform 2 at 0.125 μ M (blue line), 0.25 μ M (cyan line), 0.5 μ M (yellow line), 0.75 μ M (brown line), 1 μ M (orange line), and 2 μ M (gray line)

which were found to show diminished aggregation prevention towards different target proteins (Laganowsky et al. 2010). The same applies for human α A-crystallin isoform 1 after deletion of more than 50 residues (Kundu et al. 2007). The shortened alternative splice variant α A-crystallin isoform 2 seems to follow a similar trend.

α A-crystallin isoform 2 modulates the high oligomeric complexes of canonical α A-crystallin and α B-crystallin

Human α -crystallins assemble into large polydisperse oligomers that are able to exchange subunits. In a further set of experiments, we investigated the influence of the alternative

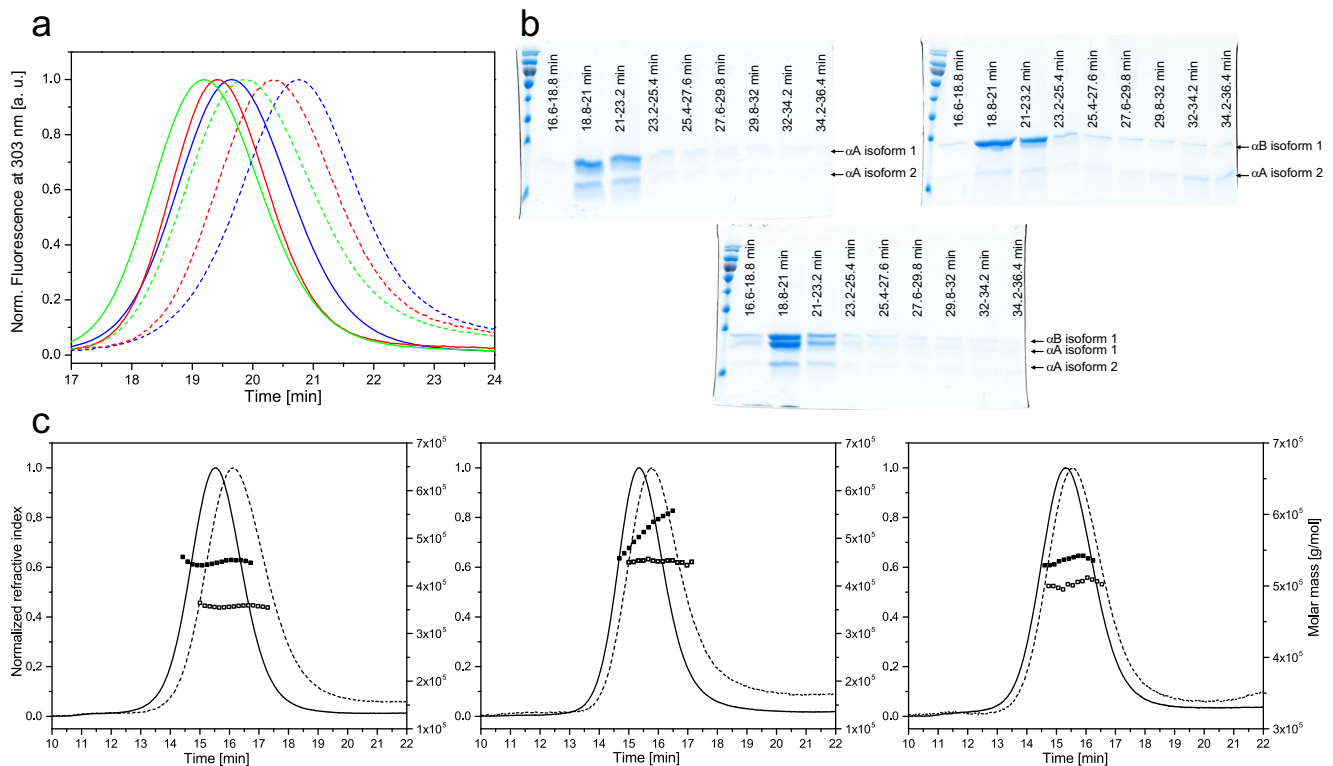


Fig. 5 Analysis of oligomer formation of α -crystallins. **a** Analytical SEC of α A-crystallin isoform 1 (blue line), α B-crystallin isoform 1 (red line), an equimolar mixture of α A-crystallin and α B-crystallin isoform 1 (green line), and the respective mixtures with α A-crystallin isoform 2 in the same colors as dashed lines. **b** Polyacrylamid gels of NaDOC/TCA precipitated fractions of the SEC runs. **c** SEC-MALS measurements of

α A-crystallin isoform 1 (left panel), α B-crystallin (middle panel), and an equimolar mixture of α A-crystallin and α B-crystallin isoform 1 (right panel) showing the normalized differential refractive index (dRI) solid line and molecular mass (g/mol) as filled squares. Dashed lines and empty squares represent the elution profiles in the presence of equimolar concentrations of α A-crystallin isoform 2

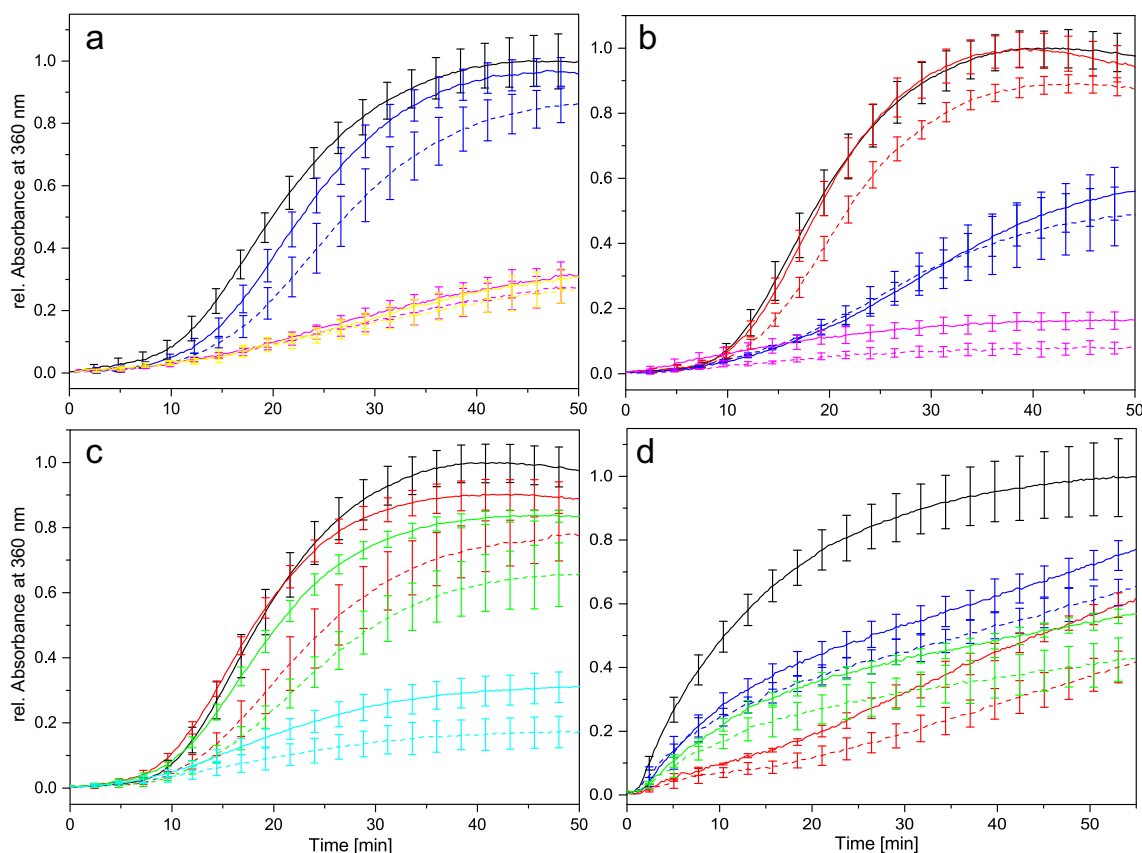


Fig. 6 Analysis of the modulating influence of α A-crystallin isoform 2 on the chaperone activity of the canonical α -crystallins. The suppression of the aggregation of MDH (**a–c**) and rhodanese (**d**) as substrates was analyzed. The spontaneous aggregation of the respective substrate alone is depicted in *black*. **a** α A-crystallin isoform 1 alone (*solid lines*) and in equimolar mixtures with α A-crystallin isoform 2 (*dashed lines*) at 0.125 μ M (*blue*), 0.375 μ M (*magenta*), and 0.5 μ M (*yellow*). **b** α B-crystallin isoform 1 alone (*solid lines*) and in equimolar mixtures with α A-crystallin isoform 2 (*dashed lines*) at 0.05 μ M (*red*), 0.125 μ M

(*blue*), and 0.375 μ M (*magenta*). **c** Equimolar mixtures of α A-crystallin and α B-crystallin isoform 1 (*solid lines*) as well as with further, equimolar addition of α A-crystallin isoform 2 at 0.05 μ M (*red*), 0.0625 μ M (*green*), and 0.25 μ M (*cyan*). **d** Aggregation of rhodanese alone (*black*) and in the presence of different canonical α -crystallins (*solid lines*) as well as with further, equimolar addition of α A-crystallin isoform 2 (*dashed lines*). α A-crystallin isoform 1 (*blue*, 0.25 μ M), α B-crystallin (*red*, 0.25 μ M), or equimolar mixtures of α A-crystallin and α B-crystallin isoform 1 (*green*, each 0.25 μ M)

splice variant of α A-crystallin on the apparent molecular size of α A-crystallin isoform 1 and α B-crystallin oligomers using size exclusion chromatography (Fig. 5a). Because the cellular ratio between the canonical isoform and α A-crystallin isoform 2 cannot be concluded from our experiments and requires further investigations, we always used equimolar concentrations of α -crystallins in mixtures to study the effect of the alternative splice variant. α A-crystallin and α B-crystallin formed large oligomers with an average of ~ 24 subunits which is in accordance with the literature (Kundu et al. 2007). Interestingly, the splice variant α A-crystallin isoform 2 was able to form hetero-oligomeric complexes with α A-crystallin isoform 1 and α B-crystallin. The mean oligomeric size of the hetero-oligomeric complexes decreased. Interestingly, the change in the apparent molecular mass cannot be solely explained by the smaller protein size of α A-crystallin isoform 2, since the amount of isoform 2 in the eluting peak is much lower than would be expected by

calculation assuming a 24mer (Fig. 5b). This indicates that the mean amount of subunits in the complex is altered as well. To verify that α A-crystallin isoform 2 indeed is incorporated in the high molecular weight complexes of α A-crystallin isoform 1 and α B-crystallin, we analyzed the peaks by SDS-PAGE (Fig. 5b). The majority of α A-crystallin isoform 2 was found to be present in the early eluting large hetero-oligomeric complexes. Interestingly, the modulation of the α B-crystallin oligomer by incorporation of α A-crystallin isoform 2 seems to be less pronounced, but still a distinct shift in the apparent molecular mass was detected. SEC-MALS measurements to determine the apparent molecular mass of the hetero-oligomeric complexes in the presence of the splice variant of α A-crystallin were conducted (Fig. 5c). Again, a decrease in the apparent molecular mass for α A-crystallin isoform 1 and α B-crystallin in case of the hetero-oligomer with the splice variant was detected.

The presence of α A-crystallin isoform 2 enhances the chaperone activity of the canonical α A-crystallins and α B-crystallins

Since α A-crystallin isoform 2 is largely devoid of chaperone activity, we were interested in determining the chaperone activity of the respective hetero-oligomers. Both canonical α -crystallins have a strong chaperone activity towards MDH and rhodanese as substrates (Mymrikov et al. 2016) and are by far more active than α A-crystallin isoform 2 (Figs. 4 and 6). At equimolar ratios of sHsp to substrate, α A-crystallin isoform 2 alone showed no protective effect on the aggregation of the substrate. However, when α A-crystallin isoform 1 and α A-crystallin isoform 2 are present together, the aggregation of MDH and rhodanese was suppressed to a higher extent than for the α A-crystallin isoform 1 alone (Fig. 6a, d). This effect is especially pronounced at low concentrations of α A-crystallin and attenuates with increasing concentration of isoform 1. Interestingly, α B-crystallin is influenced in a similar manner by α A-crystallin isoform 2 as α A-crystallin isoform 1 (Fig. 6b, d). Moreover, the splice variant of α A-crystallin is even able to modulate the chaperone activity of the hetero-complex of the canonical α A-crystallins and α B-crystallins and enhances their potential to suppress the aggregation of MDH and rhodanese (Fig. 6c, d). A similar trend was found for other human sHsps like HspB1 and HspB6 (Heirbaut et al. 2016). The large homo-complex forming HspB1 together with the dimer forming HspB6 predominantly generated hetero-oligomeric entities smaller than HspB1 alone, but with a higher apparent molecular weight than HspB6 alone. Additionally, the hetero-oligomers had an increased chaperone activity compared to the components alone (Heirbaut et al. 2016).

Conclusions

Taken together, our results verified the presence of an alternatively spliced variant of human α A-crystallin in human lens tissue. This alternative splice variant, annotated as isoform 2 in the NCBI database, has a substituted NTS that is shorter and has a high predicted total positive charge in comparison to the NTS of the canonical isoform 1 but is similar in the composition and distribution of hydrophobic amino acids. α A-crystallin isoform 2 turned out to be a soluble protein with a secondary structure typical for sHsp. According to secondary structure prediction, isoform 2 loses the two initial N-terminal helices but still carries one N-terminal helix at a similar position as the canonical α A-crystallin and α B-crystallin. In contrast to α A-crystallin isoform 1 which preferentially forms large oligomers, the alternative splice variant was found to be in a monomer–dimer equilibrium. On its own, it exhibited only low aggregation prevention activity towards heat-

induced aggregation of model substrates, which the canonical crystallins protect with ease, even at low concentrations. Nevertheless, α A-crystallin isoform 2 integrated into the high oligomeric complexes of the canonical α -crystallins and led to a decrease in the subunit number of both α A-crystallin and α B-crystallin isoform 1 oligomers. Interestingly, the hetero-oligomers of the splice variant and the canonical α -crystallins show enhanced chaperone activity. Hence, in addition to post-translational modifications, alternative mRNA splicing yields at least one additional, formerly not characterized α -crystallin species. Furthermore, this additional α -crystallin variant modulates the ensemble of oligomers. Hetero-oligomers of canonical α -crystallins and the splice variant show enhanced chaperone activity. Overall, the observed functional implications of this splice variant are likely to add a further layer of complexity on the regulation of the α -crystallin ensemble in the human eye lens.

Acknowledgments We thank Gina Feind for excellent experimental assistance, Robert Pesch and Ralf Zimmer for discussion of bioinformatics data on alternative splicing, and Evgeny Mymrikov for α B-crystallin. The Deutsche Forschungsgemeinschaft (SFB 1035) and CIPS^M are acknowledged for financial support.

References

- Bassnett S, Shi Y, Vrensen GF (2011) Biological glass: structural determinants of eye lens transparency. *Philos Trans R Soc Lond Ser B Biol Sci* 366:1250–1264. doi:10.1098/rstb.2010.0302
- Bepperling A et al (2012) Alternative bacterial two-component small heat shock protein systems. *Proc Natl Acad Sci U S A* 109:20407–20412. doi:10.1073/pnas.1209565109
- Berengian AR, Parfenova M, McHaourab HS (1999) Site-directed spin labeling study of subunit interactions in the alpha-crystallin domain of small heat-shock proteins. Comparison of the oligomer symmetry in alphaA-crystallin, HSP 27, and HSP 16.3. *J Biol Chem* 274:6305–6314. doi:10.1074/jbc.274.10.6305
- Bhat SP, Nagineni CN (1989) α B subunit of lens-specific protein α -crystallin is present in other ocular and non-ocular tissues. *Biochem Biophys Res Commun* 158:319–325. doi:10.1016/S0006-291X(89)80215-3
- Bhattacharyya J, Das KP (1998) Alpha-crystallin does not require temperature activation for its chaperone-like activity. *Biochem Mol Biol Int* 46:249–258. doi:10.1080/15216549800203762
- Bloemendal H, de Jong W, Jaenicke R, Lubsen NH, Slingsby C, Tardieu A (2004) Ageing and vision: structure, stability and function of lens crystallins. *Prog Biophys Mol Biol* 86:407–485. doi:10.1016/j.pbiomolbio.2003.11.012
- Bohm G, Muhr R, Jaenicke R (1992) Quantitative analysis of protein far UV circular dichroism spectra by neural networks. *Protein Eng* 5:191–195. doi:10.1093/protein/5.3.191
- Bonaldo MF, Lennon G, Soares MB (1996) Normalization and subtraction: two approaches to facilitate gene discovery. *Genome Res* 6:791–806. doi:10.1101/gr.6.9.791
- Bova MP, Ding LL, Horwitz J, Fung BK (1997) Subunit exchange of alphaA-crystallin. *J Biol Chem* 272:29511–29517. doi:10.1074/jbc.272.47.29511
- Bova MP, McHaourab HS, Han Y, Fung BK (2000) Subunit exchange of small heat shock proteins. Analysis of oligomer formation of

- alphaA-crystallin and Hsp27 by fluorescence resonance energy transfer and site-directed truncations. *J Biol Chem* 275:1035–1042. doi:10.1074/jbc.275.2.1035
- Braun N et al (2011) Multiple molecular architectures of the eye lens chaperone alphaB-crystallin elucidated by a triple hybrid approach. *Proc Natl Acad Sci U S A* 108:20491–20496. doi:10.1073/pnas.1111014108
- Carver JA, Aquilina JA, Truscott RJ, Ralston GB (1992) Identification by 1H NMR spectroscopy of flexible C-terminal extensions in bovine lens alpha-crystallin. *FEBS Lett* 311:143–149. doi:10.1016/0014-5793(92)81386-Z
- Clark AR, Lubsen NH, Slingsby C (2012) sHSP in the eye lens: crystallin mutations, cataract and proteostasis. *Int J Biochem Cell Biol* 44:1687–1697. doi:10.1016/j.biocel.2012.02.015
- Cohen LH, Westerhuis LW, de Jong WW, Bloemendal H (1978a) Rat alpha-crystallin A chain with an insertion of 22 residues. *Eur J Biochem* 89:259–266. doi:10.1111/j.1432-1033.1978.tb20921.x
- Cohen LH, Westerhuis LW, Smits DP, Bloemendal H (1978b) Two structurally closely related polypeptides encoded by 14-S mRNA isolated from rat lens. *Eur J Biochem* 89:251–258. doi:10.1111/j.1432-1033.1978.tb20920.x
- de Jong WW, Cohen LH, Leunissen JAM, Zweers A (1980) Internally elongated rodent α -crystallin A chain: resulting from incomplete RNA splicing? *Biochem Biophys Res Commun* 96:648–655. doi:10.1016/0006-291X(80)91404-7
- Delaye M, Tardieu A (1983) Short-range order of crystallin proteins accounts for eye lens transparency. *Nature* 302:415–417. doi:10.1038/302415a0
- Delbecq SP, Kleivit RE (2013) One size does not fit all: the oligomeric states of alphaB crystallin. *FEBS Lett* 587:1073–1080. doi:10.1016/j.febslet.2013.01.021
- Derham BK et al (2001) Chaperone function of mutant versions of alpha A- and alpha B-crystallin prepared to pinpoint chaperone binding sites. *Eur J Biochem* 268:713–721. doi:10.1046/j.1432-1327.2001.01929.x
- Dubin R, Wawrousek E, Piatigorsky J (1989) Expression of the murine alpha B-crystallin gene is not restricted to the lens. *Mol Cell Biol* 9:1083–1091. doi:10.1128/MCB.9.3.1083
- Eifert C, Burgio MR, Bennett PM, Salerno JC, Koretz JF (2005) N-terminal control of small heat shock protein oligomerization: changes in aggregate size and chaperone-like function. *Biochim Biophys Acta* 1748:146–156. doi:10.1016/j.bbapap.2004.12.015
- Fagerholm PP, Philipson BT, Lindström B (1981) Normal human lens—the distribution of protein. *Exp Eye Res* 33:615–620. doi:10.1016/S0014-4835(81)80101-7
- Fleming TP, Song Z, Andley UP (1998) Expression of growth control and differentiation genes in human lens epithelial cells with extended life span. *Invest Ophthalmol Vis Sci* 39:1387–1398
- Graw J (2009) Genetics of crystallins: cataract and beyond. *Exp Eye Res* 88:173–189. doi:10.1016/j.exer.2008.10.011
- Haslbeck M, Franzmann T, Weinfurter D, Buchner J (2005) Some like it hot: the structure and function of small heat-shock proteins. *Nat Struct Mol Biol* 12:842–846. doi:10.1038/nsmb993
- Haslbeck M, Peschek J, Buchner J, Weinkauff S (2016) Structure and function of alpha-crystallins: traversing from in vitro to in vivo. *Biochim Biophys Acta* 1860:149–166. doi:10.1016/j.bbagen.2015.06.008
- Heirbaut M et al (2016) The preferential heterodimerization of human small heat shock proteins HSPB1 and HSPB6 is dictated by the N-terminal domain. *Arch Biochem Biophys* 610:41–50. doi:10.1016/j.abb.2016.10.002
- Hendriks W, Sanders J, de Leij L, Ramaekers F, Bloemendal H, de Jong WW (1988) Monoclonal antibodies reveal evolutionary conservation of alternative splicing of the alpha A-crystallin primary transcript. *Eur J Biochem* 174:133–137. doi:10.1111/j.1432-1033.1988.tb14072.x
- Hoehenwarter W, Klose J, Jungblut PR (2006) Eye lens proteomics. *Amino Acids* 30:369–389. doi:10.1007/s00726-005-0283-9
- Horwitz J (1992) Alpha-crystallin can function as a molecular chaperone. *Proc Natl Acad Sci U S A* 89:10449–10453
- Horwitz J (1993) Proctor lecture. The function of alpha-crystallin. *Invest Ophthalmol Vis Sci* 34:10–22
- Iwaki T, Kume-Iwaki A, Goldman JE (1990) Cellular distribution of alpha B-crystallin in non-lenticular tissues. *J Histochem Cytochem* 38:31–39. doi:10.1177/38.1.2294148
- Iwaki T, Kume-Iwaki A, Liem RKH, Goldman JE (1989) α B-crystallin is expressed in non-lenticular tissues and accumulates in Alexander's disease brain. *Cell* 57:71–78. doi:10.1016/0092-8674(89)90173-6
- Jaenicke R, Slingsby C (2001) Lens crystallins and their microbial homologs: structure, stability, and function. *Crit Rev Biochem Mol Biol* 36:435–499. doi:10.1080/20014091074237
- Jakob U, Gaestel M, Engel K, Buchner J (1993) Small heat shock proteins are molecular chaperones. *J Biol Chem* 268:1517–1520
- Jaworski CJ, Piatigorsky J (1989) A pseudo-exon in the functional human alpha A-crystallin gene. *Nature* 337:752–754. doi:10.1038/337752a0
- Jehle S et al (2011) N-terminal domain of alphaB-crystallin provides a conformational switch for multimerization and structural heterogeneity. *Proc Natl Acad Sci U S A* 108:6409–6414. doi:10.1073/pnas.1014656108
- Kato K, Shinohara H, Kurobe N, Goto S, Inaguma Y, Ohshima K (1991a) Immunoreactive α A crystallin in rat non-lenticular tissues detected with a sensitive immunoassay method. *Biochim Biophys Acta* 1080:173–180. doi:10.1016/0167-4838(91)90146-Q
- Kato K, Shinohara H, Kurobe N, Inaguma Y, Shimizu K, Ohshima K (1991b) Tissue distribution and developmental profiles of immunoreactive α B crystallin in the rat determined with a sensitive immunoassay system. *Biochim Biophys Acta* 1074:201–208. doi:10.1016/0304-4165(91)90062-L
- King CR, Piatigorsky J (1983) Alternative RNA splicing of the murine α A-crystallin gene: protein-coding information within an intron. *Cell* 32:707–712. doi:10.1016/0092-8674(83)90056-9
- Kundu M, Sen PC, Das KP (2007) Structure, stability, and chaperone function of alphaA-crystallin: role of N-terminal region. *Biopolymers* 86:177–192. doi:10.1002/bip.20716
- Laganowsky A et al (2010) Crystal structures of truncated alphaA and alphaB crystallins reveal structural mechanisms of polydispersity important for eye lens function. *Protein Sci* 19:1031–1043. doi:10.1002/pro.380
- Laganowsky A, Eisenberg D (2010) Non-3D domain swapped crystal structure of truncated zebrafish alphaA crystallin. *Protein Sci* 19:1978–1984. doi:10.1002/pro.471
- Lenstra JA, Hukkelhoven MWAC, Grøneveld AA, Smits RAMM, Weterings PJJM, Bloemendal H (1982) Gene expression of transformed lens cells. *Exp Eye Res* 35:549–554. doi:10.1016/S0014-4835(82)80069-9
- Liang JN, Andley UP, Chylack LT Jr (1985) Spectroscopic studies on human lens crystallins. *Biochim Biophys Acta* 832:197–203
- Mainz A et al (2015) The chaperone alphaB-crystallin uses different interfaces to capture an amorphous and an amyloid client. *Nat Struct Mol Biol* 22:898–905. doi:10.1038/nsmb.3108
- Merck KB, De Haard-Hoekman WA, Oude Essink BB, Bloemendal H, De Jong WW (1992) Expression and aggregation of recombinant alpha A-crystallin and its two domains. *Biochim Biophys Acta* 1130:267–276. doi:10.1016/0167-4781(92)90439-7
- Merck KB, Horwitz J, Kersten M, Overkamp P, Gaestel M, Bloemendal H, de Jong WW (1993) Comparison of the homologous carboxy-terminal domain and tail of alpha-crystallin and small heat shock protein. *Mol Biol Rep* 18:209–215. doi:10.1007/BF01674432
- Mymrikov EV, Daake M, Richter B, Haslbeck M, Buchner J (2016) The chaperone activity and substrate spectrum of human small heat shock proteins. *J Biol Chem*. doi:10.1074/jbc.M116.760413

- Peschek J, Braun N, Franzmann TM, Georgalis Y, Haslbeck M, Weinkauff S, Buchner J (2009) The eye lens chaperone alpha-crystallin forms defined globular assemblies. *Proc Natl Acad Sci U S A* 106:13272–13277. doi:10.1073/pnas.0902651106
- Peschek J et al (2013) Regulated structural transitions unleash the chaperone activity of alphaB-crystallin. *Proc Natl Acad Sci U S A* 110: E3780–E3789. doi:10.1073/pnas.1308898110
- Raman B, Ramakrishna T, Rao CM (1995) Temperature dependent chaperone-like activity of alpha-crystallin. *FEBS Lett* 365:133–136. doi:10.1016/0014-5793(95)00440-K
- Raman B, Rao CM (1994) Chaperone-like activity and quaternary structure of α -crystallin. *J Biol Chem* 269:27264–27268
- Reddy GB, Reddy PY, Suryanarayana P (2001) α A- and α B-crystallins protect glucose-6-phosphate dehydrogenase against UVB irradiation-induced inactivation. *Biochem Biophys Res Commun* 282:712–716. doi:10.1006/bbrc.2001.4642
- Robinson ML, Overbeek PA (1996) Differential expression of alpha A- and alpha B-crystallin during murine ocular development. *Invest Ophthalmol Vis Sci* 37:2276–2284
- Salerno JC, Eifert CL, Salemo KM, Koretz JF (2003) Structural diversity in the small heat shock protein superfamily: control of aggregation by the N-terminal region. *Protein Eng* 16:847–851. doi:10.1093/protein/gzg102
- Schuck P (2000) Size-distribution analysis of macromolecules by sedimentation velocity ultracentrifugation and lamm equation modeling. *Biophys J* 78:1606–1619. doi:10.1016/S0006-3495(00)76713-0
- Schuck P (2003) On the analysis of protein self-association by sedimentation velocity analytical ultracentrifugation. *Anal Biochem* 320: 104–124. doi:10.1016/S0003-2697(03)00289-6
- Siezen RJ, Wu E, Kaplan ED, Thomson JA, Benedek GB (1988) Rat lens γ -crystallins. *J Mol Biol* 199:475–490. doi:10.1016/0022-2836(88)90619-5
- Srinivasan AN, Nagineni CN, Bhat SP (1992) Alpha A-crystallin is expressed in non-ocular tissues. *J Biol Chem* 267:23337–23341
- Tardieu A (1988) Eye lens proteins and transparency: from light transmission theory to solution X-ray structural analysis. *Annu Rev Biophys Biophys Chem* 17:47–70. doi:10.1146/annurev.bb.17.060188.000403
- van den Heuvel R, Hendriks W, Quax W, Bloemendal H (1985) Complete structure of the hamster alpha A crystallin gene. Reflection of an evolutionary history by means of exon shuffling. *J Mol Biol* 185:273–284. doi:10.1016/0022-2836(85)90403-6
- Wistow G et al (2002) Expressed sequence tag analysis of human retina for the NEIBank project: retbindin, an abundant, novel retinal cDNA and alternative splicing of other retina-preferred gene transcripts. *Mol Vis* 8:196–204
- Wistow GJ, Piatigorsky J (1988) Lens crystallins: the evolution and expression of proteins for a highly specialized tissue. *Annu Rev Biochem* 57:479–504. doi:10.1146/annurev.bi.57.070188.002403